

FLIGHT TEST AND CFD STUDY OF THE EFFECT OF WING BOUNDARY LAYER TRANSITION ON AILERON BALANCE

Leonardo Manfriani¹ & Xinying Liu²

¹Professor, Zurich University of Applied Sciences (ret.) ²Scientific Collaborator, Zurich University of Applied Sciences

Abstract

A production training aircraft with NACA 6-series laminar wing sections exhibited an unusual lateral trim change, with a consistent tendency to roll to the left when entering a cloud or passing through an inversion layer. It was found that this behaviour was due to small steps in the paint layer which caused an asymmetric boundary layer transition on the wings when entering the cloud because of the sudden change in Reynolds number and the presence of water droplets. This was enough to affect aileron balance because of the particular aileron design.

After smoothing out the steps in the paint coat, the unusual behaviour disappeared.

This paper presents the results of a high fidelity CFD study conducted to provide further insight in this phenomenon by simulating the effects of the paint step under different Reynolds number conditions and considering the influence of the droplets encountered in the cloud. The results confirmed the explanation proposed at the time of the event.

Keywords: boundary layer transition, laminar flow, aerodynamic control balance, CFD, flight test

1. Introduction

A particular example of a single engine turboprop aircraft operated for primary pilot training developed an uncommon roll trim behaviour. This aircraft type is fitted with manually operated flight controls and an electrically operated trim tab.

The aircraft in question needed a large amount of left aileron trim to compensate a strong right roll tendency. By adjusting the trim tabs on both ailerons, it was possible to barely pass the trim check prescribed in the maintenance flight test schedule; however, the aircraft consistently exhibited a most unusual lateral trim change, with a marked tendency to roll to the left when entering a cloud or passing through an inversion layer. The aircraft was judged by the flight instructors to be unsuitable for student pilot training and remained grounded for a long time. After several unsuccessful attempts to solve the problem one of the authors (at the time head of the aerodynamics, flight mechanics and performance group at the aircraft manufacturer) was sent to the operator's air base to investigate the roll trim problems and hopefully find a way to correct the anomalous trim behaviour.

2. Investigation of the problem

A series of geometry and rigging checks and adjustments was performed and a small asymmetry in the aileron trailing edge position was detected. It was then decided to replace the ailerons including trim and balance tabs; this reduced the right roll tendency to an acceptable level. As soon as the meteorological conditions were favourable, the so-called "cloud test" was performed. This consisted in entering a cloud at high speed (220 to 280 knots), with the aircraft trimmed in all three axes, controls free. The test pilot reported that the aircraft started to roll to the left in cloud, reaching 30 degrees of bank in several seconds. The data analysis clearly showed that the roll was caused by a slight aileron movement of a few tenths of a degree, sufficient to produce the rate of roll observed.

From anecdotal evidence, the lateral trim change when entering a cloud experienced by the aircraft in question had been observed in some occasions on other aircraft of the same type, although not to such a dramatic extent. According to the manufacturer's test pilot, when this aircraft type penetrated a cloud layer diagonally (one wing first) at high speed, the ailerons kicked back and forth briefly, but with no resultant roll in the cloud.

It was assumed that this phenomenon was due to the peculiar aileron design concept of this aircraft type, where a trailing edge "bevel" is used to closely balance the hinge moments and reduce the lateral control forces to a minimum. The mechanism by which a trailing edge bevel works is schematically shown in figure 1. When, for example, the control is deflected downward, the local increase in trailing edge angle at the bevel creates a flow separation on its upper surface. The lower surface still has attached flow, and the local pressure unbalance generates a small force that tends to reduce the hinge moment when the aileron is deflected. Even if the force is small, the large moment arm with respect to the aileron hinge results makes the bevel quite effective.

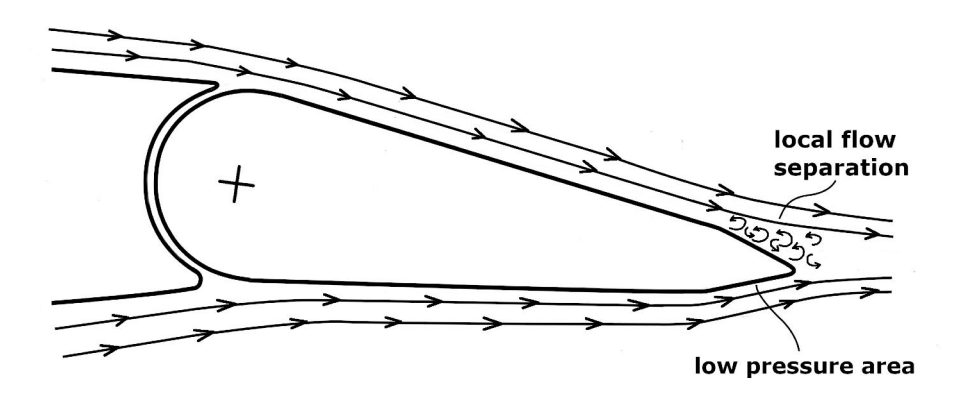


Figure 1 – Flow around a trailing edge bevel

However, the trailing edge "bevel" has the disadvantage of being very sensitive to build tolerances (small differences in the bevel angle) and to flow conditions, which are influenced by air density, humidity, and temperature as well as airspeed.

The wing of this aircraft type is built on NACA 6-series laminar airfoils and has a very high surface finish. The transition from laminar to turbulent flow is "natural" (i.e., not fixed) and varies depending on atmospheric conditions; entering a cloud can change the position of the transition line on the wing tips because of a change in temperature, humidity or density. The resulting change of boundary layer thickness at the wing trailing edge can affect the extent of flow separation on the aileron bevels. If for any reason the change in flow conditions on the wingtips does not occur symmetrically, a lateral roll force will result.

After discussing this subject with the pilot, he carefully checked the aircraft and noticed that it had a seemingly insignificant asymmetry in the paint finish on the wingtips. The right wing tip leading edge had been repainted back to the aileron gap, while the left wing tip had received a new coat of paint only on the leading edge (up to 10% of the chord). A small step could just be felt with the finger between the new and the old paint, a few hundreds of millimetres high. Although such a tiny disturbance might seem insignificant, a laminar boundary layer in high speed flow is extremely sensitive to imperfections in the surface; it was indeed possible that the step in the paint finish could trigger a transition earlier than on the other wing.

To check this idea, the aircraft was flown with a strip of aluminium tape attached to the upper surface of the right wing to simulate the paint finish step on the left wing. The flight test after this modification

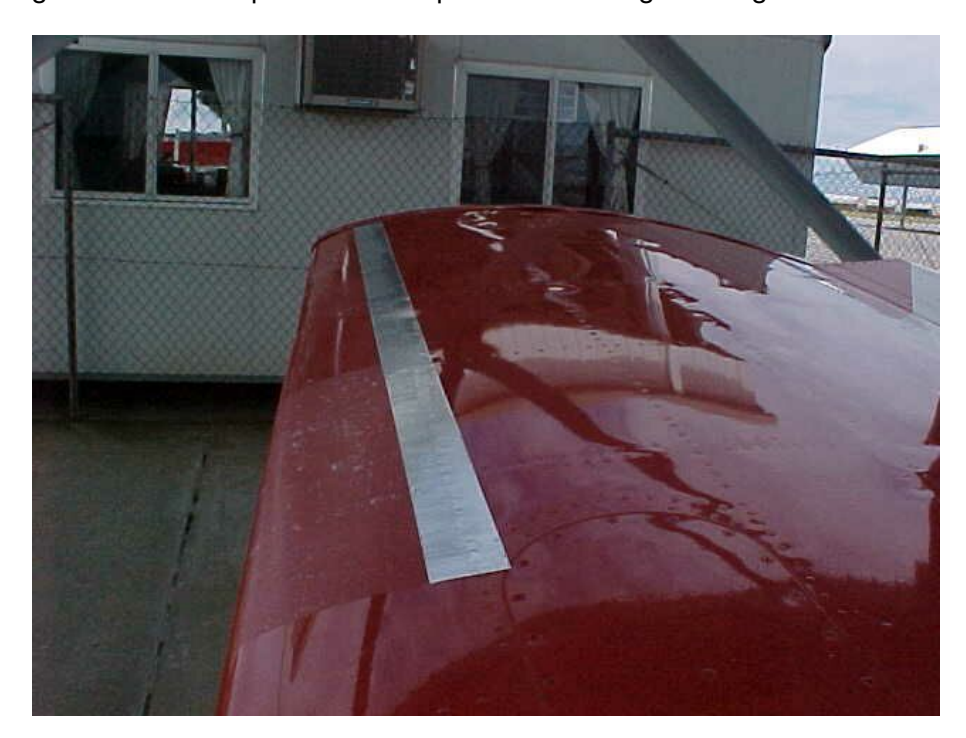


Figure 2 – Simulation of a paint step on the wing leading edge by aluminium tape

confirmed the theory: no lateral trim change was present anymore when entering a cloud layer at any speed!

The next step was to remove the tape and to carefully eliminate the step in the paint finish on the left wing with fine grain sandpaper and a cutting compound.

Again, the flight test results were very positive: there was no sign of a rolling tendency when entering a cloud. The conclusion was that the small step on the paint finish on the left wing leading edge was sufficient to cause the boundary layer to become turbulent earlier than on the right wing (which was smooth) in certain conditions. This was the cause of the curious trim change experience when entering a cloud.

The aim of this work was to reproduce the empirical results of the flight test by performing high fidelity CFD simulation of the boundary layer transition on the outer wing section wing in different atmospheric conditions, at different flight speeds and in presence of small surface steps at various chord positions. Particular attention was dedicated to the effect of boundary layer thickness on the flow separation on the upper part of the control surface bevel and its consequent effect on hinge moments. This provided a very interesting insight on the details of the boundary layer flow on a real aircraft wing in operational conditions and the mechanism by which a control surface bevel can reduce hinge moments.

3. Numerical methodology and Setup

3.1 Overview of the numerical simulation

To study the particular effect described above we carried out 2D Navier-Stokes simulations to investigate the flow field on the outer wing section with the aileron. By following a reverse engineering approach, we derived boundary conditions which were used for the simulation campaign to represent the test flight conditions as accurately as possible. The numerical investigation focused on the effect of the paint step on laminar-turbulent transition and on the effect of the transition location on the control surface bevel under real test conditions.

We started with one-phase air flow simulation to analyse the transition in "dry-air" condition as a reference. Further, we conducted multi-phase droplet-laden flow simulations, including droplet/vapour contents to simulate clouds. The compressible flow solver Ansys Fluent [2] was used for one-phase flow simulations. The results from Ansys Fluent were further processed in DROP3D, a 3D Eulerian water droplets/ice crystal impingement module of the Ansys FENSAP system [3].

Because Ansys FENSAP is a 3D solver, we carried out 2.5D simulations by extruding the 2D grids in the spanwise direction and defining the top and bottom surfaces of the cylindrical domain as "symmetry walls".

3.2 Pre-Processing

Geometry. To represent the geometry of the test airplane, we digitised the original sketches provided by the manufacturer and implemented data from measurements performed on the test airplane. To study the various effects, we tested three basic geometry configurations, as shown in figure 3:

- I. Clean: original laminar NACA airfoil with measured aileron shroud gaps, without bevel.
- II. Paint finish step: $\delta_{step} = 0.1 or 0.2$ mm backward step, corresponding to the thickness of the aluminum tape applied on the wing upper surface, without bevel.
- III. Paint finish step plus bevel: both paint finish step and bevel included.

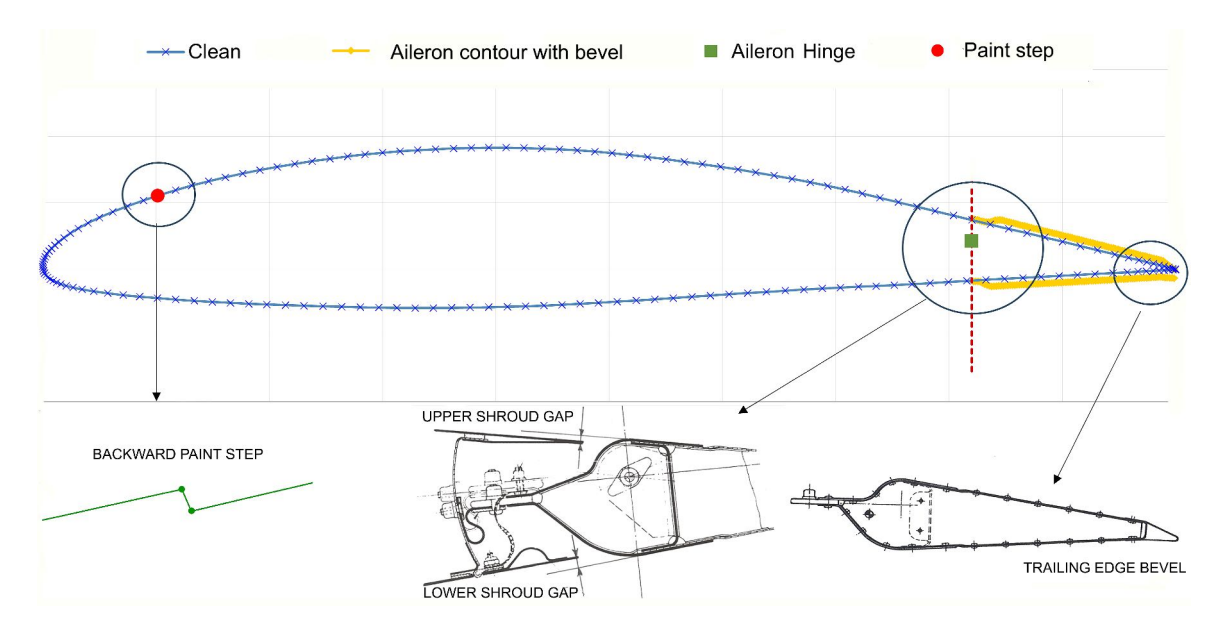


Figure 3 – Representation of the geometry details of the wing section with aileron

Grid generation and topology. We used structured O-grids with a farfield boundary condition for the flow computation. The single-block grids were generated using the commercial grid-generation tool Pointwise.

Parameter	Coarse	Medium	Fine	Very fine
Chord length	1			
farfield distance	> 300			
Streamwise spacing $\Delta x_{min}/\delta_{step}$	0.5	0.2	0.1	0.05
Y+ dimensionless wall distance	< 0.5			
Number of Cells	≈ 50000	≈ 100000	≈ 180000	≈ 260000

Table 1 – Grid parameters

Boundary layers undergoing transition are more sensitive to grid resolution than fully ones, especially in the streamwise direction. In our grid-independence study, we used a fixed value of 10^{-6} m for the first wall cell thickness and varied the streamwise spacing Δx , particularly in the regions of paint finish step, where boundary layer transition can be triggered, and aileron shroud gaps, where the flow field is complex. The key grid parameter is the ratio between minimal spacing $\Delta x_{\min}/\delta_{\text{step}}$.

Based on best practices[4], the averaged spacings of all tested grids are smaller than the empirical values of the boundary layer thickness $\delta_{0.99}$. The grid parameters are listed in table 1.

3.3 Governing equations and physics

ANSYS Fluent uses a finite-volume scheme to solve the Reynolds-Averaged Navier-Stokes (RANS) equations. The air flow is treated as compressible ideal gas. For a viscous laminar flow, the viscosity is defined empirically by Sutherland's law. In the present study, we also carried out multi-phase droplet-laden flow simulations.

ANSYS FENSAP-ICE package solves particle flow as a continuum with the Eulerian formulation [3]. The general Eulerian two-fluid model consists of the Navier-Stokes equations augmented by the particle continuity (eq.1) and momentum (eq.2) equations

$$\frac{\partial \alpha}{\partial t} + \vec{\nabla} \cdot \left(\alpha \vec{V}_d \right) = 0 \tag{1}$$

$$\frac{\partial \left(\alpha \vec{V}_{d}\right)}{\partial t} + \vec{\nabla} \left[\alpha \vec{V}_{d} \otimes \vec{V}_{d}\right] = \frac{C_{D} \operatorname{Re}_{d}}{24K} \alpha \left(\vec{V}_{a} - \vec{V}_{d}\right) + \alpha \left(1 - \frac{\rho_{a}}{\rho_{d}}\right) \frac{1}{Fr^{2}}$$
(2)

where the variables α and V_d are the mean field values of the particle concentration and droplet velocity, respectively.

The first term on the right-hand-side of the momentum equation represents the drag acting on particles of droplet mean diameter d. It is proportional to the relative particle velocity (index a refers to air), its drag coefficient C_D and the droplets Reynolds number Re_d can be calculated as follows:

$$C_D = (24/\text{Re}_d) (1 + 0.15\text{Re}_d^{0.687}) \text{ for } \text{Re}_d \le 1300$$

 $C_D = 0.4 \text{ for } \text{Re}_d > 1300$ (3)

$$\operatorname{Re}_{d} = \frac{\rho_{a} dV_{a,\infty} \left\| \vec{V}_{a} - \vec{V}_{d} \right\|}{u_{a}} \tag{4}$$

where the variables μ and ρ are viscosity and density, respectively. K represents an inertial parameter related to the freestream air velocity. The second term represents buoyancy and gravity forces, it is proportional to the Froude number Fr. In addition, we enabled the vapour transport equation, which simulates the mass and energy transfer between vapour and droplets.

3.4 Transition turbulence model

We used the Intermittency transition model (known as three-equation γ transition model) which proved more robust for our engineering application than the four-equation $\gamma - Re_{\theta}$ transition model. The latter one solves an additional transport equation Re_{θ} , which depends strongly on the freestream velocity. This strong dependence does not match the observations, since, the peculiar aircraft behaviour when entering a cloud was observed in a wide range of airspeeds.

In ANSYS, the γ transition model is compatible with multi-phase flows and combined also with the two equation turbulence model $k-\Omega-SST[7]$. The eddy/laminar viscosity ratio is used to compute the initial turbulent viscosity coefficient when starting the calculation. For flows in freestream using a farfield boundary, the eddy/laminar viscosity ratio can be reduced to 10^-5 from the default value 1 and turbulence intensity is set to 0.0008 [3].

3.5 Boundary Conditions

Air flow conditions. We defined the outer boundary of the O-grids as a "pressure farfield" with a static pressure $P=5.9\times10^4$ Pa (corresponding to a flight altitude of 14000 ft) and a temperature $T_{\rm ref}=275.9$ K (corresponding to ISA $+16^{\circ}$ C conditions). The Mach number range was Ma=0.34-0.44, corresponding to a true airspeed range between 220 and 280 knots. The corresponding Reynolds number based on the wing section chord of 1.15 m varied between 5.6 and 7.2 millions. A typical value of the local wing section lift coefficient C_l of 0.25 was estimated by a simple vortex lattice calculation based on flight test data.

Droplets reference conditions. The flight test campaign was conducted during summer days. Since no dedicated meteorological information was recorded, we took some reference values from literature [5, 6]. Furthermore, due to the complexity of droplet-laden flow, the "real" conditions have been simplified and standardised. Complex physical phenomena such as droplet kinematics, deformation and non-linear interactions of drop splash are beyond the scope of the present study. For all simulations discussed in this paper, the median volume diameter (MVD) of the monodisperse cloud droplets is $20~\mu m$. Liquid water content (LWC) is $1~g/m^3$.

3.6 Simulation execution

Three simulation campaigns were carried out with the following emphases:

- **Grid-indepence study**: Four grids were tested at $Re = 5.6 \times 10^6$ and $Re = 7.2 \times 10^6$. The geometry with a backward paint step on the leading edge was used.
- One-phase air flow simulation: Configurations with a clean surface and with a backward paint step were tested using suitable grid sizes. This aimed to study the effect of the paint step on transition.
- **Multi-phase droplet-laden flow simulation**: This aimed to replicate atmospheric conditions on the test day and study the effect of boundary layer thickness on the control surface bevel.

4. Results and discussion

4.1 Grid-independence study

We conducted a grid-independence study with the paint step airfoil configuration without bevel (see table 1) at $Re = 5.6 \times 10^6$ and $Re = 7.2 \times 10^6$. These Reynolds numbers correspond to flight speeds of 220 and 280 KTAS at 14000 ft, respectively. As the main interest of the study is to investigate the paint step impact on laminar-turbulent transition, we evaluated the aerodynamic performance of the airfoil and the skin friction coefficient C_f on the airfoil upper surface.

Grid size	$Re = 5.6 \times 10^6$		$Re = 7.2 \times 10^6$		
	C_l [-]	C_d [-]	C_l [-]	C_d [-]	
Coarse	0.25980	0.00962	0.26056	0.00965	
Medium	0.25673	0.00722	0.24612	0.00859	
Fine	0.25727	0.00572	0.24302	0.00793	
Very fine	0.25725	0.00572	0.24304	0.00793	

Table 2 – Grid-independence study: aerodynamic coefficients.

Table 2 summarises the lift and drag coefficients C_l and C_d of the airfoil at both Reynolds numbers. Figure 4 and Figure 5 show the C_f distributions at $\mathrm{Re} = 5.6 \times 10^6$ and $\mathrm{Re} = 7.3 \times 10^6$, respectively. At $\mathrm{Re} = 5.6 \times 10^6$, the lift coefficient deviation between the grids "very fine" and "coarse" is less than 1% and can be explained by the different transition predictions between the two grids. The C_d converges

using the "fine" grid. Looking at the C_f plot, it can be seen that the "fine" and "very fine" grids agree on the prediction of the transition point. On this basis, the "fine" grid was chosen for the study .

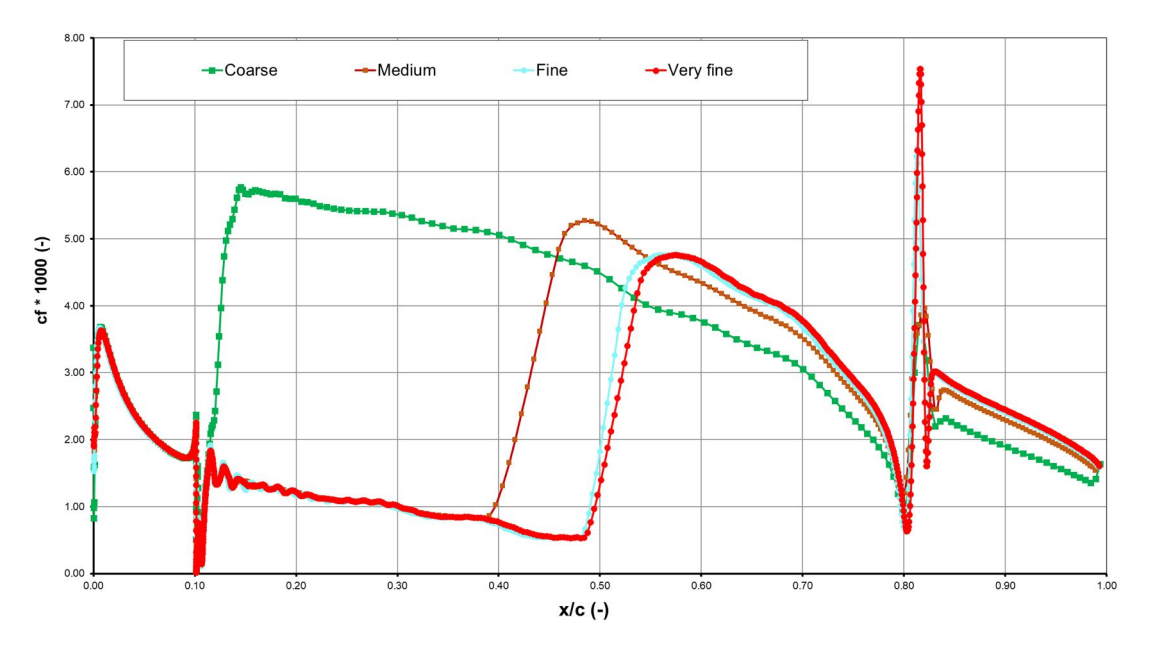


Figure 4 – Skin friction coefficient plot with 0.2 mm paint step and no trailing edge bevel. One-phase air flow at $Re = 5.6 \times 10^6$ (220 KTAS, 14000 ft, ISA +15).

At the higher Reynolds-number ${\rm Re}=7.2\times 10^6,\, C_d$ converges using the "fine" grid.. The corresponding C_f plot shows that the transition trigger due to the step at $x/c\approx 0.1$ is predicted by all grids.

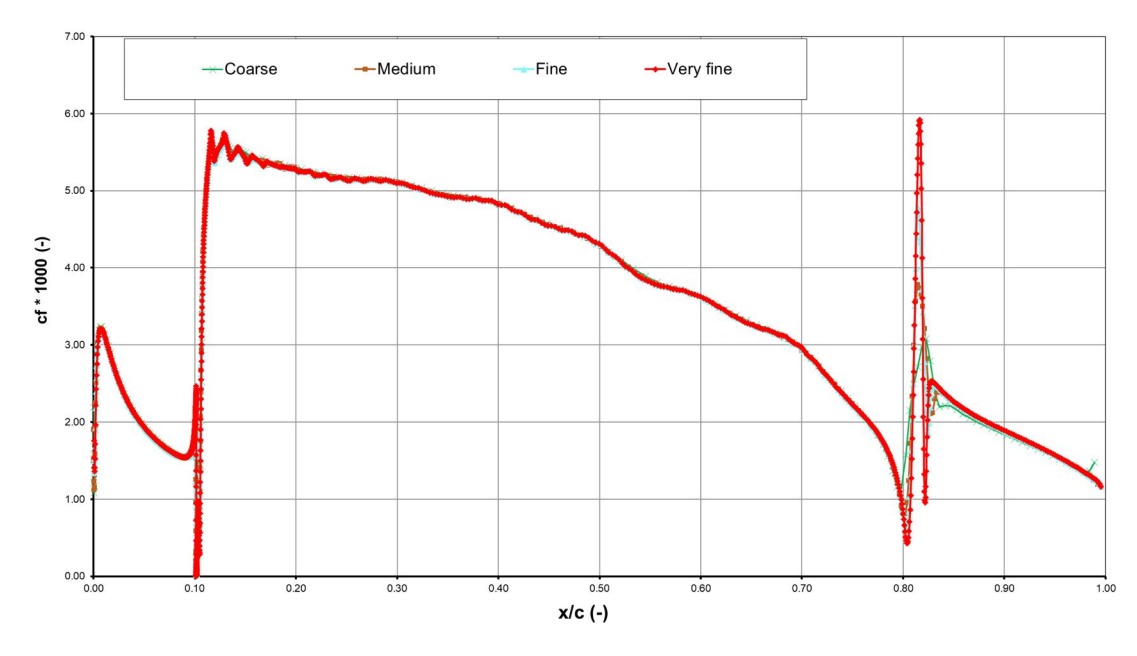


Figure 5 – Skin friction coefficient plot with 0.2 mm paint step and no trailing edge bevel. One-phase air flow at $Re = 7.2 \times 10^6$ (280 KTAS, 14000 ft, ISA +15).

4.2 Main study

In the main study, we evaluated different aspects that can influence transition and aerodynamic loads on the trailing edge bevel of the aileron, which was assumed to be the cause of the roll trim problem observed in flight test.

To study the effect of the step on the transition point, we carried out a series of simulations using the clean and paint step configurations (with 0.1 mm and 0.2 mm steps) in "dry-air" conditions (one-

phase air flow) at two different Reynolds numbers. Furthermore, we enabled the droplet and vapour models to simulate the aerodynamic behavious of the wing section in clouds.

Figure 6 compares the skin frictions distributions of the clean and paint step configurations at $Re = 5.6 \times 10^6$ and $Re = 7.2 \times 10^6$. As found in the previous grid-independence study, the combination of an increased Reynolds number and the presence of a step causes an earlier transition with respect to the natural transition on the upper surface of the clean configuration.

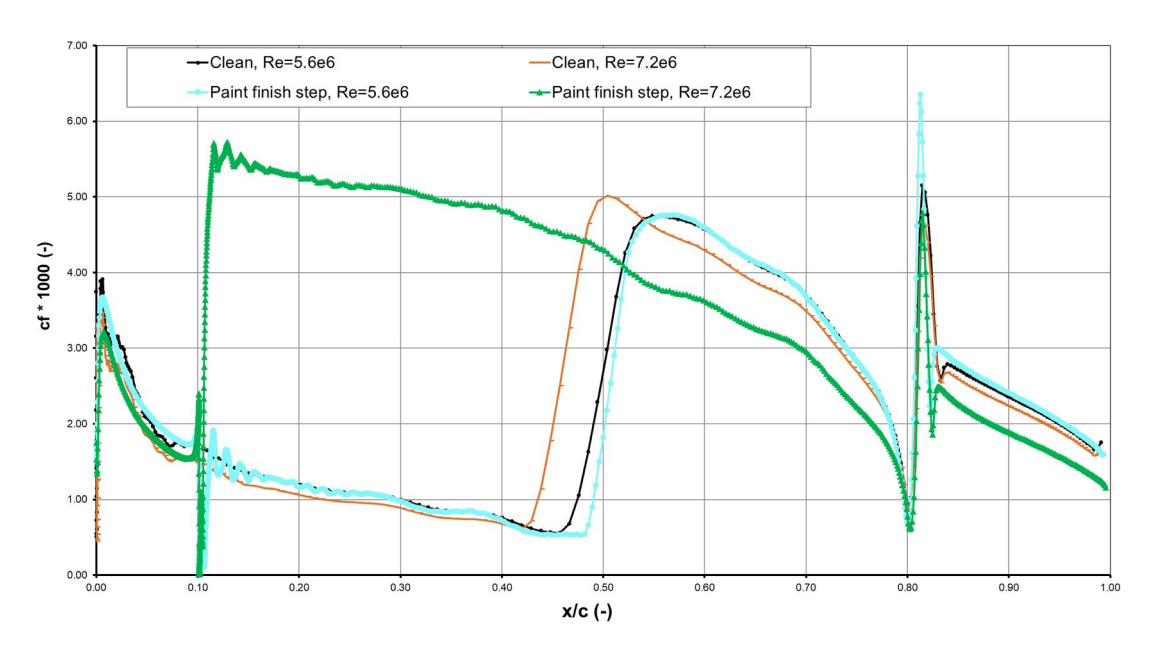


Figure 6 – Skin friction coefficient plots, clean and with paint step, no trailing edge bevel.

One-phase air flow.

The thickness of the aluminum tape applied to the wing during one of the last flight tests was in the range of 0.1 - 0.5 mm. To evaluate the effect of step height, we conducted further one-phase airflow simulations using a modified airfoil with the optimal mesh spacing derived from the grid-independence study. Figure 7 presents the results.

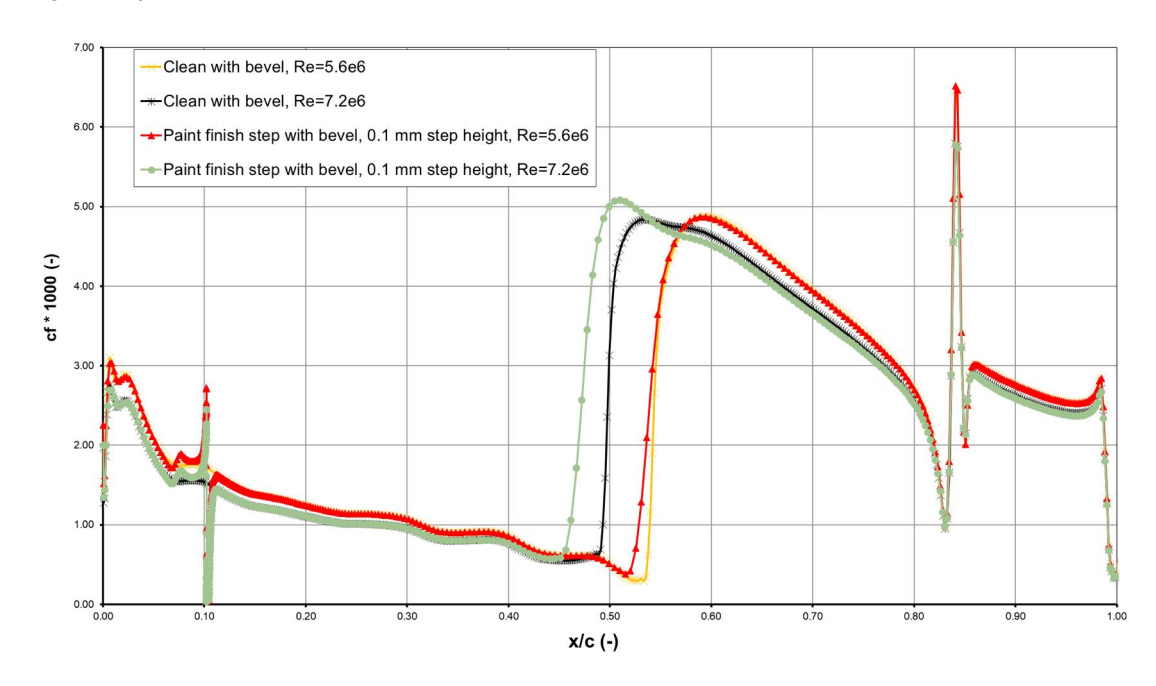


Figure 7 – Skin friction coefficient plots, clean and with paint step, with trailing edge bevel.

One-phase air flow.

With a reduced step height, free transition at both Reynolds numbers can be observed. The results of the one-phase airflow show that the late natural transition typical of NACA 6-series laminar wind sections can be achieved, however, it is sensitive to the Reynolds numbers and surface smoothness.

Further, we investigated the laminar airfoil using a multi-phase flow solver to reproduce the empirical results of flight tests. Our focus was on studying the upper part of the bevel and its impact on hinge moments, using configurations with the bevel in this simulation round. Figure 8 presents the skin friction coefficients for the tested configurations under various environmental conditions.

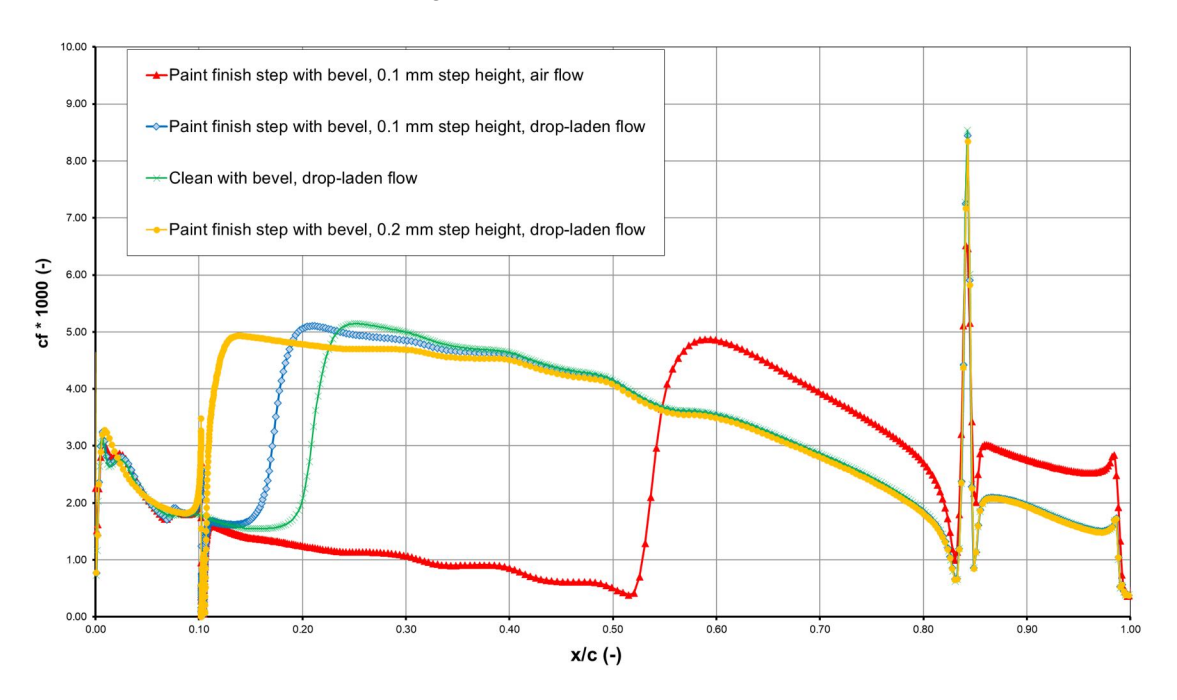


Figure 8 – Skin friction coefficient plots, clean and with paint step, with trailing edge bevel. One-phase air flow and droplet-laden flow at $Re = 5.6 \times 10^6$..

For simplicity, we assumed that the droplets are uniform in size and mass (monodisperse). The results demonstrate that the presence of droplets can trigger an earlier transition. As a "worst-case" scenario, early transition occurs even at $Re = 5.6 \times 10^6$.

Compared to the surface skin friction in "dry-air" conditions, the skin friction on the aileron is lower, observed in both clean and painted configurations. This reduction is due to fully developed turbulent flow near the bevel, where the energy redistribution mechanism decreases shear stress and frictional drag. Figure 9 shows streamlines and velocity distributions, confirming findings from flight tests that no flow separation was present on the aileron surface up to the bevel. However, control deflection does cause flow separation on the upper surface of the bevel. The resulting local pressure imbalance at the trailing edge generate a force that can compensate hinge moments during aileron deflection. Quantitatively, it is evident that "wet" conditions amplify pressure imbalances. To calculate the dimensionless hinge moment coefficient due to the bevel, we used approximately 2% of the chord length as the reference length. Table 8 provides an overview of the absolute values of hinge moment contributions due to the bevel for different paint step configurations in "dry" and "wet" environments.

Configuration Environment	Clean	Step height 0.1 mm	Step height 0.2 mm
Dry air flow	0.0418	0.0420	0.0392
Droplet-laden flow	0.0597	0.0596	0.0596
$\Delta [\%]$	42.668	41.827	51.944

Table 3 – Hinge moment coefficient contribution of the bevel at $Re = 5.6 \times 10^6$.

Under "wet" conditions, these hinge moment contributions increase by approximately 40-50%, significantly affecting roll trim and controllability. These quantitative values support previous arguments that "wet" conditions reinforce flow separation.

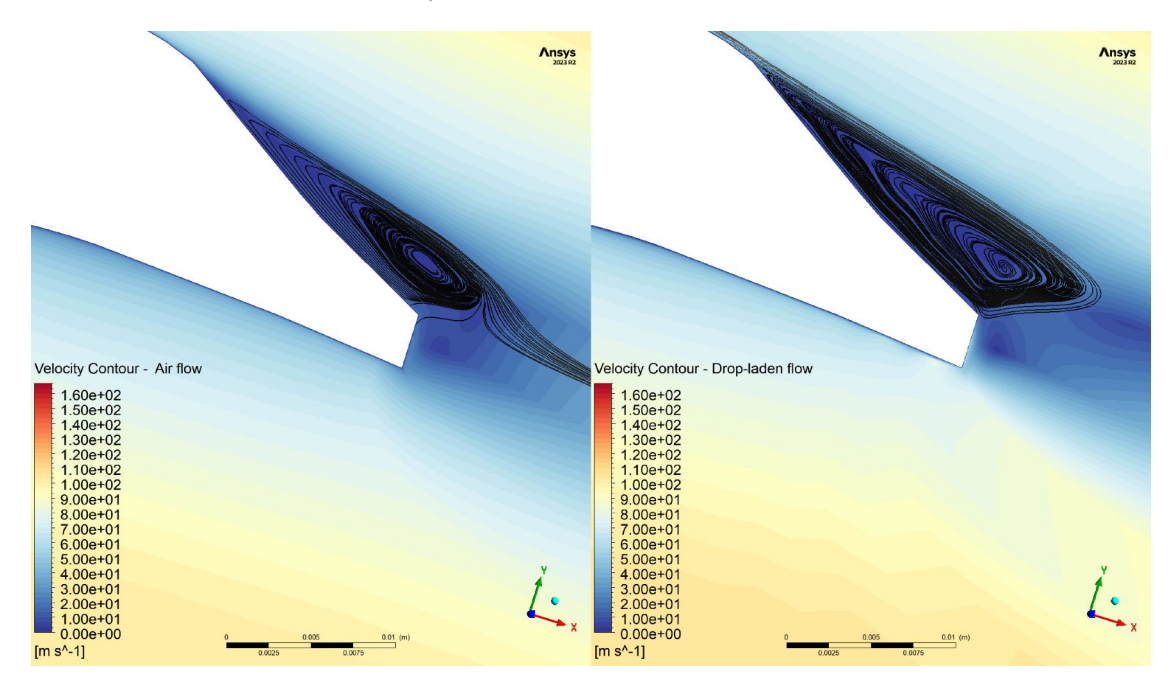


Figure 9 – Velocity distributions and streamlines on the upper surface of the bevel.

5. Conclusions

A production training aircraft exhibited an unusual lateral trim change, with a consistent tendency to roll to the left when entering a cloud or passing through an inversion layer. An extensive flight test investigation showed that this behaviour was caused by small steps in the paint layer which caused an asymmetric transition on the wings when entering the cloud because of the sudden change in Reynolds number and free stream turbulence conditions. This was enough to affect the balance of the ailerons. After smoothing out the steps in the paint coat, the unusual behaviour disappeared.

To provide further insight in this phenomenon we conducted several CFD simulation rounds using the outboard wing section with different configurations under "dry-air" and "wet-air" conditions. The skin friction distribution on the upper surface was extensively studied. The transition can be affected by a combination of Reynolds number, presence of droplets, and the smoothness (step height) of the airfoil surface. The investigation is not comprehensive and does not precisely represent environmental conditions because of lack of exact meteorological information. Nevertheless, it confirms the hypothesis that the asymmetrical paint step can cause lateral trim problems when entering a cloud.

The calculations show that the trailing edge bevel is indeed very effective in reducing hinge moments due to control deflection but is quite sensitive to boundary layer development, particularly because of changes in the transition location.

It is also confirmed that the wing of this aircraft, although of conventional riveted metal construction, can maintain laminar flow up to 50% of the chord if the high quality of the finish is maintained.

6. Contact information

Leonardo Manfriani: I.manfriani@me.com

Xinying Liu: liux@zhaw.ch

7. Copyright Statement

The authors confirm that they, and/or their company or organisation, hold copyright on all of the original material included in this paper. The authors also confirm that they have obtained permission, from the copyright holder of any third party material included in this paper, to publish it as part of their paper. The authors confirm that they give permission, or have obtained permission from the copyright holder of this paper, for the publication and distribution of this paper as part of the ICAS proceedings or as individual off-prints from the proceedings.

References

- [1] Jones R T and Ames M B A. Wind tunnel investigation od control-surface characteristics. V -The use of a beveled trailing edge to reduce the hinge moment of a control surface. *NACA Wartime Report*, L-464, 1942.
- [2] Ansys, Inc. Ansys Fluent User Manual. Ansys, Inc., 2023.
- [3] Ansys, Inc. Ansys FENSAP-ICE User Manual. Ansys, Inc., 2023.
- [4] Menter F, Sechner R and Matyushenko A. *Best Practice: RANS Turbulence Modeling in Ansys CFD.* Ansys Germany GmbH and NTS Russia, 2021.
- [5] Wu Z. Deformation and breakup of water droplets near an airfoil leading edge. *Advances in Colloid and Interface Science*, Vol. 256, pp 23-47, 2018.
- [6] Vargas M and Feo A. Deformation and breakup of water droplets near an airfoil leading edge. *Journal of Aircraft*, Vol. 48, No. 5, pp 1749-1765, 2011.
- [7] Menter F. Two-equation eddy-viscosity turbulence models for engineering applications. *AIAA Journal*, Vol. 32, pp 1598-1605, 1994.